Metal Ion Binding and Enzymatic Mechanism of *Methanococcus jannaschii* RNase HII†

Bing Lai, Ying Li, Aoneng Cao, and Luhua Lai*

State Key Laboratory for Structural Chemistry Studies of Stable and Unstable Species, Institute of Physical Chemistry, College of Chemistry, Peking University, Beijing 100871, China

Received October 7, 2002; Revised Manuscript Received November 21, 2002

ABSTRACT: RNase H degrades the RNA moiety in DNA:RNA hybrid in a divalent metal ion dependent manner. It is essential to understand the role of metal ion in enzymatic mechanism. One of the key points in this study is how many metal ions are involved in the enzyme catalysis. Accordingly, either one-metal binding mechanism or two-metal binding mechanism is proposed. We have studied the thermodynamic properties of four metal ions (Mg^{2+}, Mn^{2+}, Ca^{2+}, and Ba^{2+}) binding to *Methanococcus jannaschii* RNase HII using isothermal titration calorimetry. All of the four metal ions were found to bind Mj RNase HII with 1:1 stoichiometry in the absence of substrate. Together with enzymatic activity assay data, we propose that only one metal ion binding to the enzyme in catalytic process. We also studied the pH dependence of metal binding and enzyme activity and found that at pH 6.5, Mg^{2+} did not bind to the enzyme without the substrate but still activated the enzyme to about 2% of its maximum activity (in 10 mM Mn^{2+} at pH 8). This implies that the substrate may also be incorporated in metal ion binding and help to position the metal ion. To find which acidic residues correspond to metal ion binding, we also studied the binding thermodynamics and enzymatic activity assay of four mutants: D7N, E8Q, D112N, and D149N in the presence of Mn^{2+}. The thermodynamic parameters are least affected for the D149N mutant, which has a very low enzymatic activity. This indicates that Asp149 is essential for the enzymatic activity. On the basis of all these observations, we suggest a metal binding model in which D7, E8, and D112 bind the metal ion and D149 activates a water molecule to attack the P−O bond in the RNA chain of the substrate.

RNase His a kind of nuclease that specifically degrades the RNA moiety in DNA:RNA hybrid leaving 5′-phosphate and 3′-hydroxyl termini in a divalent metal ion dependent way (*1*, *2*). RNase H exists in a variety of organisms from human to archaea (*3*−*5*). Some studies show that RNase H is involved in the removal of the primer in the Okazaki fragment during DNA replication (*4*, *6*). The highly conserved structure in RNase H family, the so-called RNase H domain, also plays important role in many RNase H-domain-containing retroviruses, including HIV-1[1] reverse transcriptase (*7*). Some other proteins, such as HIV-1 integrase catalytic domain (*8*), RuvC Holliday junction resolvase (*9*), avian sarcoma virus integrase catalytic domain (*10*), and bacteriophage Mu transposase core (*11*), are structurally similar with RNase H fold. This makes it important to understand the mechanism of RNase H enzymatic activity.

RNase H family has two important members: type I and type II, which have very low sequence homology but high structural similarity (*12*). *Methanococcus jannaschii* RNase HII belongs to type II RNase H group that shares noticeable sequence similarity with human major RNase H. It is composed of two domains, and the larger domain is structurally homologous with *Escherichia coli* RNase HI (*13*).

Two alternative mechanisms have been proposed for enzymatic activity of *E. coli* RNase HI. One mechanism involves one metal ion in the catalytic process and activates a water molecule to attack the scissile phosphate of the RNA (*14*, *15*). And the other mechanism is based on the 3′-5′ exonuclease mechanism of DNA polymerase I which involves two metal ions (*16*). Recently Susan Marqusee's group proposed an activation/attenuation mechanism in which the first Mn^{2+} activates the enzyme and the second one attenuates the enzyme's activity (*17*).

Compared with *E. coli* RNase HI, which belongs to type I RNase H group, we know less about type II RNase H. Thus, our work on metal binding properties to Mj RNase HII should provide more information for understanding catalytic mechanism of type II RNase H. Isothermal titration calorimetry is a powerful method of determining the interaction between metal ions and proteins (*18*, *19*). For example, Cowan's group has studied Mg^{2+} binding to *E. coli* RNase HI (*20*) and Mn^{2+} and Mg^{2+} binding to HIV−1 reverse transcriptase (*21*) by using ITC. And they found that both *E. coli* RNase HI and HIV−1 reverse transcriptase RNase H domain bind one Mg^{2+}; however, HIV−1 reverse transcriptase RNase H domain binds two Mn^{2+} ions. Here, we

† This work has been supported by the National Natural Science Foundation of China (No. 29525306, No. 20173001), and the Ministry of Science and Technology of China. The earlier work related to Mj RNase HII is supported by NIH Grant GM62412 (awarded to Sung-Hou Kim, University of California, Berkeley).

* Corresponding author. Tel.: +86 10 62757486. Fax: +86 10 62751725. E-mail address: lhlai@pku.edu.cn.

[1] Abbreviations: HIV-1, human immunodeficiency virus 1; Mj, *Methanococcus jannaschii*; BME, 2′-mercaptoethanol; WT, wild type; CD, circular dichroism; ITC, isothermal titration calorimetry.

10.1021/bi026960a CCC: $25.00
Published on Web 12/28/2002

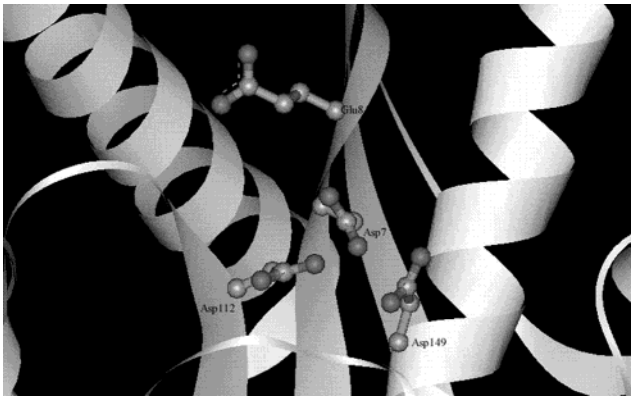

FIGURE 1: Metal ion binding site of Mj RNase HII. The four acidic residues are illustrated. Figure generated by ViewerLite 5.0 of Accelrys Inc. (http://www.accelrys.co).

use ITC combined with enzyme activity assay and protein engineering as our major tools. Our preliminary work showed that Mn^{2+}, Mg^{2+}, and Ca^{2+} bind to Mj RNase HII with 1:1 ratio at pH 8.0 (*22*). We have extended this study to four metal ions: Mg^{2+}, Mn^{2+}, Ca^{2+}, and Ba^{2+} and also at acidic pH. We find that all the four metal ions bind to the enzyme with 1:1 ratio. Our enzyme activity assay data imply a single metal ion binding mechanism.

The pH dependence of metal ion binding and activity of the enzyme has also been studied, and we find that at pH 6.5, the enzyme does not bind Mg^{2+} but can be activated by Mg^{2+}. This observation indicates that the substrate and the metal ion have some kind of interaction, although the detailed description of this interaction needs further study.

It has been proposed that four acidic residues constitute the metal binding site of *Mj* RNase HII (Figure 1). However, no evidences indicate that all these four acidic residues directly bind the metal ion. Brian R. Chapados and co-workers proposed that in *Archaeoglobus fulgidus* RNase HII, only three acidic residues bind the metal ion and the other one plays a role in catalytic process (*23*). Qing Chai and co-workers studied the metal dependent enzymatic activity of *Archaeoglobus fulgidus* RNase HII and proposed that Asp129 may participate in the second metal binding for activity inhibition (*24*). To understand the role of the four acidic residues in Mj RNase HII, four mutants are constructed, and their binding thermodynamics with Mn^{2+} have been studied. We compared the thermodynamic data and the enzymatic activity of these four mutants with the wild-type enzyme and proposed a metal ion binding model for RNase HII in catalytic process.

MATERIALS AND METHODS

Materials. Poly A was purchased from Sigma. dT_{36} was synthesized by Sangon Biotechnology Co. (Shanghai). *E. coli* RNase HI was purified according to reference (*25*). All the other reagents are of analytical grade. All the water used after protein purification was of Milli-Q grade. Site-directed mutation kit is from StrataGene.

Expression and Purification of RNase HII. Expression vector pET 21a containing Mj RNase HII gene is transformed to host strain BL21(DE3)/pSJS1244. Cells are cultivated in Luria broth (LB) containing 50 μg ml^{-1} Ampicillin and 50 μg ml^{-1} Spectinomycin at 37 °C. When the O.D. at 600 nm reaches 0.8, 0.5 mM IPTG is added. After 2 h induction, cells are collected and dispersed in 50 mM TrisHCl, pH 7.5, 10% sucrose, 0.5 mM PMSF, and 3 mM BME and sonificated. Soluble fraction is collected and heated at 80 °C for 30 min. Then the solution is centrifuged at 10 000*g* for 20 min. The supernatant is loaded on a cation exchange column Hitrap SP (Amersham biotech.). Chromatography buffer is 50 mM sodium phosphate, pH 6.9, 3 mM BME, 1 mM EDTA. Protein is eluted by a linear gradient of 0−1M NaCl. Protein elutes at about 0.3 M NaCl (*13*). Protein concentration is determined by UV absorbance. $A_{280}^{0.1\%}$ is obtained by Bradford method to be 0.654. Bovine serum albumin is used as standard protein. The $A_{280}^{0.1\%}$ value is also calculated to be 0.713 according to the method suggested by C. Nick Pace (*26*). These two values have a deviation within 10%, and the value obtained from Bradford method is used. Mutants are assumed to have the same extinction coefficient as the WT.

Site-Directed Mutagenesis. Four acidic residue mutants, D7N, E8Q, D112N, and D149N, are constructed using the Quick Change site directed mutagenesis kit box from StrataGene. Amino acid coding is AAC for Asn and CAG for Gln. Correctness of mutation is verified by sequencing.

Metal Ion Elimination. About 1 mL of purified and concentrated protein is diluted in 15 mL buffer containing 20 mM TrisHCl, pH 8.0, 50 mM NaCl, 3 mM BME, 10 mM EDTA. Then the solution is ultrafiltered by Ultrafree-15 (MWCO 5000, Millipore) to a final volume of <1 mL. This procedure is repeated for three times. The final solution goes through a Sephadex G-25 (Amersham Biotech.) desalting column. To eliminate possibly existing EDTA, the protein is ultrafiltered by Ultrafree-15 for three times in 20 mM TrisHCl, pH 8.0, 50 mM NaCl, 3 mM BME. At pH 6.5 and 5.5, Bis-TrisHCl and MES is used instead of TrisHCl, respectively.

Isothermal Titration Calorimetry. Calorimetric titration is done on a model 4200 isothermal titration calorimeter from Calorimetry Science Corp. All the experiments are done at 25 °C with stirring speed of 100 rpm. A 0.8 mL protein solution is put in the cuvette. Protein concentrations are as follows: at pH 8.0, $MnCl_2$ titration 0.51 mM, $MgCl_2$ titration 0.76 mM, $CaCl_2$ titration 0.68 mM, and $BaCl_2$ titration 0.49 mM; at pH 6.5, $MnCl_2$ titration 0.64 mM. Divalent metal ion solution is prepared by direct dissolving an appropriate amount of dichloride salt in titration buffer (20 mM TrisHCl, pH 8.0, or 20 mM Bis-TrisHCl, pH 6.5, 50 mM NaCl, 3 mM BME) and put in a 250 μL titration buret. Metal ion concentration is 10−20-fold that of protein concentration. Each titration injects 8 μL divalent metal ion solution, and the time between two injections is 400 s. Twenty-five aliquots are injected in total. Data are collected with the instrument's accompanying software and processed with BindWorks 1.0b of Applied Thermodynamics.

Enzymatic Activity Assay. The RNase HII substrate used is PolyA:dT_{36}, which is prepared as follows: about 33 μg of dT_{36} is dissolved in 490 μL of buffer, and 20 μL of 4 mg/mL PolyA is added. Then the mixture is heated at 80 °C for 20 min and cooled slowly to ensure correct base pair match. Substrate concentration is represented by deoxythymine mononucleotide concentration. dT concentration is measured by UV absorbance with extinction coefficient ϵ_{260} of 9.67×10^3 M^{-1} cm^{-1} obtained from phosphate assay (*27*).

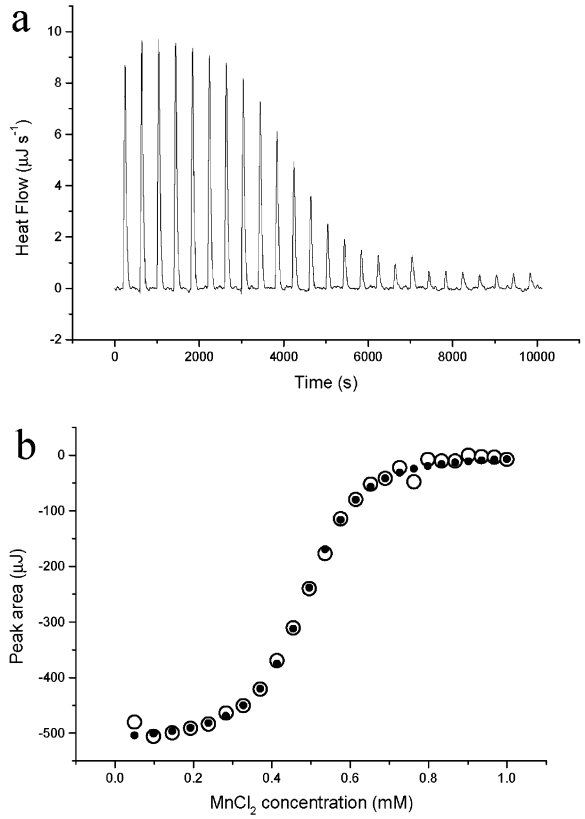

FIGURE 2: Calorimetric titration curve and curve fitting of Mn^{2+} to Mj RNase HII at pH 8.0. The experiment is done in 20 mM TrisHCl, pH 8.0, 50 mM NaCl, 3 mM BME. Open circles: experimental data. Closed circles: curve fitting. (a) Titration curve of 5 mM $MnCl_2$ titrated to 0.51 mM protein. (b) Curve fitting of 5 mM $MnCl_2$ titrated to 0.51 mM protein.

This substrate is similar to that of Black and Cowan (*28*), and *E. coli* RNase HI is used as a standard to ensure this substrate to be a proper substrate of RNase H. Enzymatic reaction is initiated by manually mixing the enzyme and the substrate. Enzymatic activity is observed by the UV absorbance increase at 260 nm when the enzyme is breaking P−O bond to leave adenine accessible to water (*28*). UV signal slope in the first 30 s is taken as the initial rate. Kinetic data is obtained by fitting the initial rate data to Michaelis−Menten equation:

$$V = \frac{[S]\cdot V_m}{[S] + K_m}$$

where V is initial velocity, [S] is substrate concentration, V_m is maximum velocity, and K_m is Michaelis−Menten constant. None-linear curve fit is done by MicroCal Origin 5.0.

RESULTS

Divalent Metal Ion Binding Thermodynamics at pH 8.0. The preliminary results for Mj RNase HII binding with three types of metal ions have been reported in our previous paper (*22*). Here we have studied the binding of four types of divalent metal ions: Mn^{2+}, Mg^{2+}, Ca^{2+}, and Ba^{2+}. Figure 2 illustrates titration curve and the fit of data when Mn^{2+} is titrated as representative. All these four divalent metal ions are capable of binding to Mj RNase HII with a ratio of 1:1. Thermodynamic parameters are listed in Table 1. Entropy change ΔS is calculated with the following form:

Table 1: Thermodynamics of Divalent Metal Ions Binding to Mj RNase HII

metal ion	pH	binding number n	association constant K_a	ΔH (kJ mol^{-1})	ΔS (J K^{-1} mol^{-1})
Mn^{2+}	8.0	1.04	7.9×10^4	−12.9	50
	6.5	0.87	4.5×10^3	−2.4	62
Mg^{2+}	8.0	0.91	7.1×10^3	−7.0	50
Ca^{2+}	8.0	0.92	8.7×10^3	−7.5	50
Ba^{2+}	8.0	1.02	6.7×10^2	−8.7	25

$$\Delta S = \frac{\Delta H + RT \ln K_a}{T}$$

where ΔH is enthalpy change, K_a is association constant, T is temperature, and R is the gas constant. All the metal ion binding thermodynamics show a relatively small exothermic heat from −7.0 to −12.9 kJ mol^{-1}. Mn^{2+} has the largest association constant with Mj RNase HII. While Mg^{2+} and Ca^{2+} have similar association constants, Ba^{2+} binds the enzyme with a very small association constant. Interestingly, Mn^{2+}, Mg^{2+}, and Ca^{2+} have the same ΔS upon binding. This implies that these metal ions may bind to the enzyme in the same way.

The interpretation of binding enthalpy and entropy can be complicated when binding accompanies protonation/deprotonation process. The protonation/deprotonation process involves proton transfer from/to the buffer. In this case, the buffer protonation enthalpy will affect the detected binding enthalpy. Since we do our ITC study only in one kind of buffer and do not compare the ΔH value in various buffers, the ΔH and ΔS value may only be regarded as apparent. At pH 8.0, it seems this is not a big problem because the side chain of Asp and Glu have pK_a values of around 4. Although in proteins the pK_a value can vary by as large as 2, the four metal binding residues should be fully ionized at pH 8.0. And the binding process is not coupled with deprotonation. At pH 6.5, this is a problem. It is possible that the four acidic residues are not totally ionized and our ΔH and ΔS values are apparent. However, this complication should not affect the comparison of thermodynamic parameters among mutants as they were all studied at pH 8.0.

Divalent Metal Ion Binding Thermodynamics at pH 6.5. To illustrate how carboxylate group protonization can influence metal ion binding, titration is also done at pH 6.5. Three metal ions, Mn^{2+}, Mg^{2+}, and Ca^{2+}, are titrated. At this pH, only Mn^{2+} can still bind with a much smaller heat release and association constant, while Mg^{2+} and Ca^{2+} do not show distinct binding. The curve fitting and result are shown in Figure 3. We also tried titration of Mn^{2+} at pH 5.5. A very weak binding was observed (data not shown).

Metal Binding Property of the Mutants. Thermodynamic properties of the four mutants binding with Mn^{2+} are measured by ITC. The thermodynamic data are listed in Table 2. Most of the mutants preserve metal binding ability although weakened. Association constants decrease from 7.9×10^4 of WT to 5.3×10^3 of D7N, 2.0×10^3 of E8Q, and 9.8×10^3 of D149N. Metal binding ability totally disappears when Asp112 is mutated to Asn. The binding constant is least affected by D149N. Binding entropy has a distinct

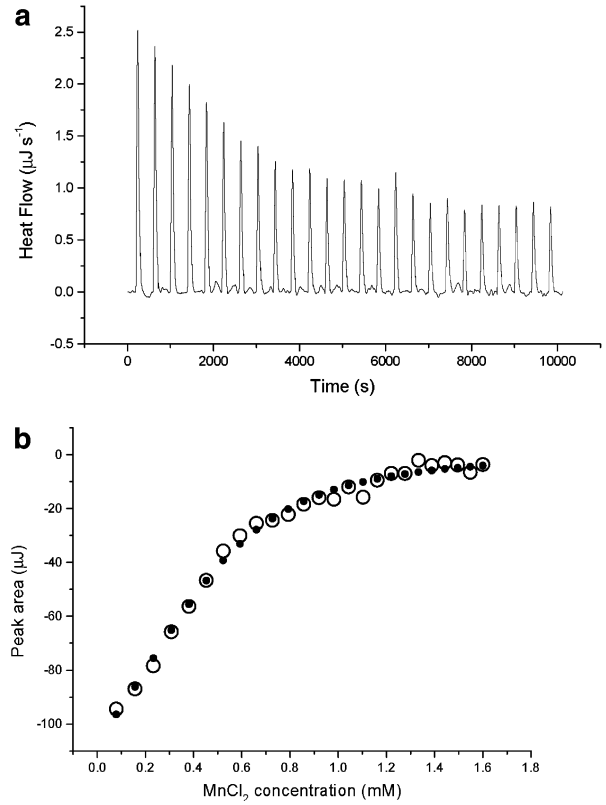

FIGURE 3: Calorimetric titration curve and curve fitting of Mn^{2+} to Mj RNase HII at pH 6.5. Titration buffer is 20 mM Bis-TrisHCl, pH 6.5, 50 mM NaCl, 3 mM BME. Open circles: experimental data. Closed circles: curve fit. (a) Titration curve of 8 mM $MnCl_2$ titrated to 0.64 mM protein. (b) Curve fitting of 8 mM $MnCl_2$ titrated to 0.64 mM protein.

Table 2: Thermodynamics of Mn^{2+} Binding to Mj RNase HII Mutants

	binding number n	binding constant K	enthalpy change ΔH (kJ mol^{-1})	entropy change ΔS (J K^{-1} mol^{-1})
WT	1.03	7.9×10^4	−12.9	50
D7N	0.84	5.3×10^3	−24.3	−10
E8Q	0.97	2.0×10^3	7.0	86
D112N	0	0		
D149N	0.87	9.8×10^3	−6.1	56

variation among the mutants. D149N changes from 50 to 56 J K^{-1} mol^{-1}, while D7N changes to −10 J K^{-1} mol^{-1} and E8Q to 86 J K^{-1} mol^{-1}. In D149N, the binding enthalpy decreases to −6.1 kJ mol^{-1}, and this is a relatively small change compared to the other two mutants. The data imply that D149N has the same metal binding mode as wild type and Asp149 does not directly bind to the metal ion.

Enzymatic Activity Assay. Since Mj RNase HII activity has not been tested on the substrate we used, it is necessary to identify its enzymatic kinetics. Dependence of initial velocity on substrate concentration is shown in Figure 4. The kinetics agrees with Michaelis−Menten mechanism. And the kinetic parameters are listed in Table 3. It is shown that Mj RNase HII catalyzes neither PolyA nor dT_{36}. Enzymatic activity of Mj RNase HII and *E. coli* RNase HI in 50 mM NaCl are also listed in Table 3.

At first, we find too small a K_m value in 50 mM NaCl to be obtained accurately. To solve this problem, we use a higher salt concentration to reduce the interaction between the nucleic acid and the protein. 500 mM NaCl, which can increase K_m to a measurable level, is added to enzyme activity assay buffer.

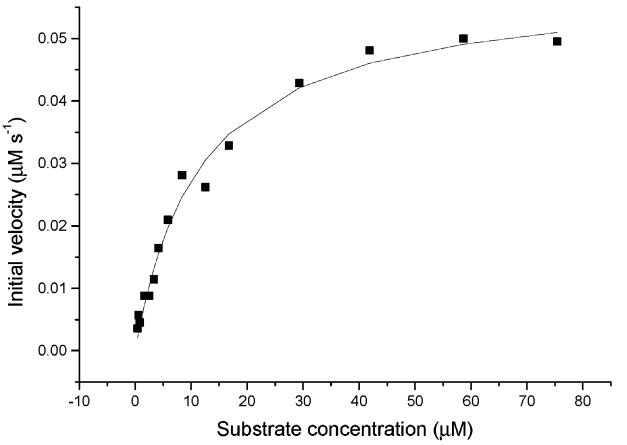

FIGURE 4: Variation of initial velocity against substrate concentration changes. Activity assay buffer is 20 mM TrisHCl, pH 8.0, 500 mM NaCl, 3 mM BME. Final Mj RNase HII concentration is 0.52 μM.

Table 3: Kinetic Parameters of Mj RNase HII

enzyme	substrate	K_m (μM)	k_{cat} (s^{-1})[a]
Mj RNase HII[b]	PolyA:dT_{36}	11.6 ± 1.3	0.11 ± 0.01
Mj RNase HII[b]	PolyA		0
Mj RNase HII[b]	dT_{36}		0
Mj RNase HII[c]	PolyA:dT_{36}		0.64 ± 0.04
E. coli RNase HI[c]	PolyA:dT_{36}		4.9 ± 0.2

[a] k_{cat} is calculated by $k_{cat} = V_{max}/[E]$. [b] Activity assay buffer is 20 mM TrisHCl, pH 8.0, 500 mM NaCl, 3 mM BME, 10 mM $MgCl_2$. Final Mj RNase HII concentration is 0.52 μM. [c] Activity assay buffer is 20 mM TrisHCl, pH 8.0, 50 mM NaCl, 3 mM BME, 10 mM $MgCl_2$. Final Mj RNase HII concentration is 0.5 μM. Final *E. coli* RNase HI concentration is 0.05 μM.

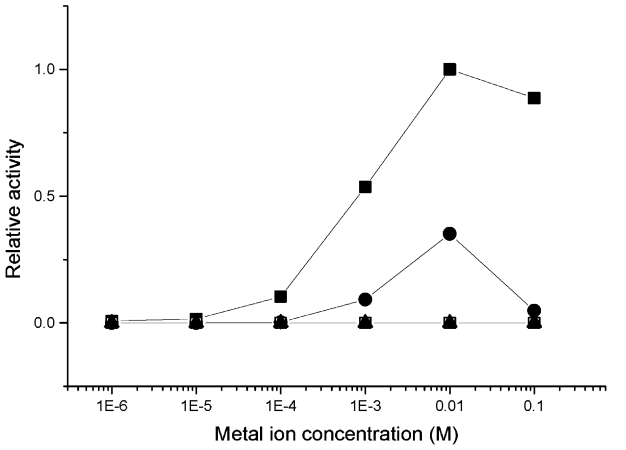

FIGURE 5: Metal ion dependence of Mj RNase HII activity. Enzymatic activity assay is performed in 20 mM TrisHCl, pH 8.0, 50 mM NaCl, 3 mM BME, 48 μM PolyA:dT_{36}, 0.50μM Mj RNase HII. Closed square, $MnCl_2$; closed circle, $MgCl_2$; open square, $CaCl_2$; triangle, $BaCl_2$.

Metal-Dependent Activity of Mj RNase HII. We vary metal ion concentration to see the metal ion concentration dependence of the enzymatic activity. Figure 5 shows RNase HII activity at various metal ion concentrations.

Our metal ion concentration dependent enzymatic activity assay illustrated that Ca^{2+} and Ba^{2+} do not facilitate catalytic reaction at any concentration. Mj RNase HII has activity

Table 4: pH Dependence of Activity[a]

pH	activity in 10 mM Mn^{2+}	activity in 10 mM Mg^{2+}
8.0	100	54 ± 5
6.5	58 ± 3	2.0 ± 0.7
5.5	0	0

[a] Activity assay buffer is 50 mM NaCl, 3 mM BME, and 20 mM TrisHCl for pH 8.0, 20 mM Bis-TrisHCl for pH 6.5, and 20 mM MES for pH5.5. Final Mj RNase HII concentration is 0.5 μM. Activity in 10 mM Mn^{2+} at pH 8 is set to 100.

Table 5: Relative Activity of Mutants[a]

enzyme	relative activity
WT	100
D7N	0.13 ± 0.04
E8Q	0.14 ± 0.05
D112N	0.17 ± 0.09
D149N	0.12 ± 0.03

[a] Activity assay buffer is 20 mM TrisHCl, pH 8.0, 50 mM NaCl, 3 mM BME, 10 mM $MnCl_2$. WT activity is set to 100.

when Mg^{2+} or Mn^{2+} exists with a little difference. Either of them has low activity in low concentration and higher activity when concentration increases. They all cause the highest activity at about 10 mM. But when the concentration is higher, activity in Mg^{2+} decreases rapidly and in Mn^{2+} decreases only a little. The enzyme is more active with Mn^{2+} than with Mg^{2+} at each concentration.

pH Dependence of the Activity. We did activity assay in the same divalent metal ion concentration at pH 8, 6.5, and 5.5 to examine the pH dependence of the activity. The result is listed in Table 4. At pH 5.5, neither Mn^{2+} nor Mg^{2+} can activate the enzyme. And at pH 6.5, Mn^{2+} recovers about half of the activity at pH 8. At this pH, Mg^{2+} shows weak but observable activity. Taking account that the enzyme cannot bind Mg^{2+} at pH 6.5 as illustrated by ITC, we propose that the substrate should interact with the metal ion and help to position it.

Activity Assay of Mutants. The enzymatic activities of RNase HII mutants in the presence of 10 mM Mn^{2+} are assayed (Table 5). We cannot determine the K_m value of each mutant enzyme because the activity of all the four mutants are lower relative to the WT and the K_m value cannot be determined accurately. Our results are similar with the results obtained by Ayumu Muroya and co-workers on *Thermococcus kodakaraensis* KOD1 RNase HII (*29*), that enzymatic activity is strongly depressed in all the mutants.

DISCUSSION

Enzymatic Activity Assay. For the first time, we have studied Mj RNase HII reaction kinetics, and it agrees with Michaelis−Menten mechanism. A small K_m is observed which cannot be obtained accurately in physiological ionic strength. This is not surprising because *Methanococcus jannaschii* lives at an optimal temperature of 85 °C, and at 25 °C the interaction between nucleic acid and the enzyme should be stronger. Specific activity of the enzyme in hyperthermophiles is generally lower than that of the corresponding enzyme in mesophiles (*30*). This can explain the experimental result that Mj RNase HII has specific activity about $^1/_8$ that of *E. coli* RNase HI under the same conditions (Table 3).

Metal Ion Binding of Mj RNase HII and Metal-Dependent Enzymatic Activity. RNase H family degrade the RNA moiety in DNA:RNA duplex in a divalent metal ion dependent manner. However, the role of metal ion in the catalytic reaction is still under debate. How many metal ions bind to the enzyme remains unclear. *E. coli* RNase HI is the most thoroughly studied model enzyme in RNase H family. A variety of methods have been used, and either one metal ion mechanism (*14*, *15*) or two metal ion mechanism (*16*) is proposed. A recent crystallography study of Goedken and Marqusee proposed a model that *E. coli* RNase HI can bind only one Mg^{2+} ion but two Mn^{2+} ions, and the second Mn^{2+} binding will inhibit enzyme activity (*31*). Until now, few studies have been reported on the mechanism of type II RNase H. Although Mj RNase HII has one domain that is structurally similar with *E. coli* RNase HI, their metal-dependent catalytic mechanism should not presumably be the same.

Isothermal titration calorimetry is the only tool that can obtain all the thermodynamic parameters in binding process (*32*). This makes it a suitable method to illustrate the thermodynamics during metal binding. Our ITC study reveals that metal ion binds to Mj RNase HII with a 1:1 stoichiometry. This agrees with the one metal ion mechanism in *E. coli* RNase HI. It is a bit surprising that all the four divalent metal ions have the ability to bind the enzyme although only two of them (Mg^{2+}, Mn^{2+}) are cofactors of the enzyme. This wide binding ability and limited enzymatic activity may imply that the enzyme binds divalent ions mainly by electrostatic interaction but enzymatic activity needs more criteria.

Goedken and Marqusee proposed a good model to explain the activation/attenuation behavior of Mn^{2+} in *E. coli* RNase HI (*31*). They observed that Mn^{2+} only activated the enzyme at low concentrations over a narrow range (to ~2 μM), and additional metal prohibited the enzyme. However, this is not the case for Mj RNase HII. Mn^{2+} does not show any inhibition effects contrasting the strong inhibition with high concentration of Mn^{2+} in *E. coli* RNase HI (Figure 5). But Mg^{2+} has a high concentration inhibition profile similar to that of *E. coli* RNase HI. This high concentration inhibition may be caused by the strong interaction between Mg^{2+} and the DNA:RNA substrate, which interferes the enzymatic process. This concentration-dependent activity profile indicates that in Mj RNase HII, the metal ion may not play the same role as in *E. coli* RNase HI and implies that in the catalytic process, still only one metal ion is bound.

Interaction Between Substrate and Metal Ion. The metal ion binding ability of Mj RNase HII strongly dependents on the pH of the solution. At pH 6.5, only Mn^{2+} can bind to the enzyme, while Mg^{2+} and Ca^{2+} cannot. This might caused by the protonation at the metal binding site. Mn^{2+} has a stronger interaction with the binding site than the other two types of metal ions, so it can still bind to the metal binding site at lower pH. Surprisingly, although the enzyme cannot bind Mg^{2+} at pH 6.5, it still preserves a noticeable activity (~2% of the activity in 10 mM Mn^{2+} at pH 8) in the presence of 10 mM Mg^{2+}. The possible explanation is that the substrate provides a part of metal ion binding ability. Thus an enzyme−substrate−metal ion complex may exist. This is further confirmed by mutational analysis on D112N. This mutant cannot bind Mn^{2+} at the observable level, while it

has a considerable high activity among all the four mutants. The details of substrate's facilitation and its role in catalysis need further study.

Metal Ion Binding Mode. Although thermodynamic study cannot derive the structural details of the metal ion binding to the enzyme directly, we can still obtain much information from thermodynamic parameters. It is assumed from crystallography and mutational study that three acidic residues have the potential to bind metal ion in *E. coli* RNase HI (*14*, *15*, *33*, *34*). Brian R. Chapados and co-workers proposed that three acidic residues, Asp6, Glu7, and Asp101, are involved in metal binding in *Archaeoglobus fulgidus* RNase HII and the other acidic residue, Asp129, activates a water molecule to attack the substrate (*23*). They did structural superposition on *Archaeoglobus fulgidus* RNase HII and Mj RNase HII and found these residues to correspond to Asp7, Glu8, Asp112, and Asp149, respectively. However, their assumption is proposed only on the basis of mutant activity assay without further evidence.

We notice that the entropy changes of Mn^{2+}, Mg^{2+}, and Ca^{2+} upon binding to the wild type are all approximately 50 J K^{-1} mol^{-1}. It seems that this is not just by chance. There must be a unique way to determine the entropy change during binding. Mn^{2+} has association constant and enthalpy change much larger than the other two ions, but it has the same entropy change. This implies that all these three metal ions bind the enzyme in a same manner.

The metal binding scenario is further illustrated by mutational analysis. We suppose that the substitution of the carboxyl group to carboxylamide group should only affect the local electrostatic property but not the total structure of the protein. And this assumption is supported by CD spectroscopy (data not shown). Thermodynamic study on the three mutants, D7N, E8Q, and D149N, shows that all the three mutants preserve metal binding property, although weakened. The loss of binding strength may come from the loss of electrostatic attraction while the carboxyl group is changed to carboxylamide group. Only the D112N mutant loses metal binding ability totally, which indicates that D112 definitely binds to the metal ion in the active site. Compared to the other three mutants, D149N has a different set of thermodynamic parameters. It has a binding entropy of 56 J mol^{-1} K^{-1}, which is very close to the binding entropy of the WT. This implies that D149 does not directly form a bond with metal ion, so D149N does not affect the metal binding mode much compared to the WT. According to enzymatic activity assay which shows that D149N's activity is strongly decreased compared to the WT, D149 should be involved in the catalytic process. Considering that its position is very close to the other acidic residues, the most probable way it acts is to activate a water molecule that is bound by the metal ion. Thus, we propose an enzymatic mechanism in Figure 6 in which the metal ion is bound by Asp7, Glu8, and Asp112 while a water molecule is positioned by the metal ion and forms a hydrogen bond with Asp149 and the P−O bond in the RNA moiety of the substrate is attacked by this water molecule. This metal binding mode agrees with Brian R. Chapados' proposal.

Our thermodynamic study and activity assay of metal ion binding to Mj RNase HII and its mutants are informative in understanding its enzymatic mechanism. This is important because many retroviral duplications involve RNase H activity. However, the direct structural description of the substrate−enzyme complex is difficult due to its low solubility (*35*, *36*), so little is known about the metal binding, substrate recognition and enzymatic mechanism. To fully understand the enzymatic mechanism and the substrate recognition mechanism, more thermodynamic, kinetic, structural, and mutational work needs to be done.

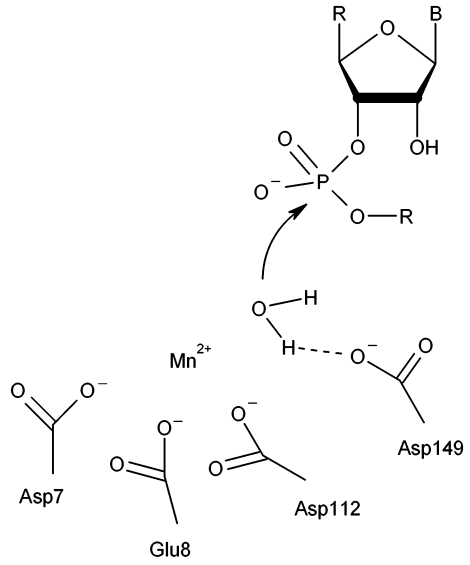

FIGURE 6: Schematic representation of the role of metal ion in catalysis. Mn^{2+} represents the metal ion.

ACKNOWLEDGMENT

The early work on Mj RNase HII was started in Professor Sung-Hou Kim's laboratory at the Univeristy of California at Berkeley when LH Lai was a Berkeley Scholar there. We thank Dr. S.-H. Kim, Dr. R. Kim, and members of the Kim lab for their encouragement, discussions, and support. We thank Dr. Shigenori Kanaya for his kindly providing *E. coli* RNase HI overproducer.

REFERENCES

1. Stein, H., and Hausen, P. (1969) *Science 166*, 393−395.
2. Cathala, G., Rech, J., Huet, J., and Jeanteur, P. (1979) *J. Biol. Chem. 254*, 7361.
3. Frank, P., Braunshofer-Reiter, C., Wintersberger, U., Grimm, R., and Busen, W. (1998) *Proc. Natl. Acad. Sci. U.S.A. 95*, 12872−12877.
4. Frank, P., Braunshofer-Reiter, C., Karwan, A., Grimm, R., and Wintersberger, U. (1999) *FEBS Lett. 450*, 251−256.
5. Ohtani, N., Haruki, M., Morikawa, M., Crouch, R. J., Itaya, M., and Kanaya, S. (1999) *Biochemistry 38*, 605−618.
6. Turchi, J. J., Huang, L., Murante, R. S., Kim, Y., and Bambara, R. A. (1994) *Proc. Natl. Acad. Sci. U.S.A. 91*, 9803−9807.
7. Davies, J. F., II., Hostomska, Z., Hostomsky, Z., Jordan, S. R., and Matthews, D. A. (1991) *Science 252*, 88−95.
8. Dyda, F., Hickman, A. B., Jenkins, T. M., Engelman, A., Craigie, R., and Davies, D. R. (1994) *Science 266*, 1981−1986.
9. Ariyoshi, M., Vassylyev, D. G., Iwasaki, H., Nakamura, H., Shinagawa, H., and Morikawa, K. (1994) *Cell 78*, 1063−1072.
10. Bujacz, G., Jaskolski, M., Alexandratos, J., Wlodawer, A., Merkel, G., Katz, R. A., and Skalka, A. M. (1996) *Structure 4*, 89−96.
11. Rice, P., and Mizuuchi, K. (1995) *Cell 82*, 209−220.
12. Ohtani, N., Haruki, M., Morikawa, M., and Kanaya, S. (1999) *J. Biosci. Bioeng. 88*, 12−19.
13. Lai, L., Yokota, H., Huang, L., Kim, R., and Kim, S. (2000) *Structure 8*, 897−904.
14. Katayanagi, K., Okumura, M., and Morikawa, K. (1993) *Proteins Struct. Funct. Genet. 17*, 337−346.

15. Kanaya, S., Oobatake, M., and Liu, Y. (1996) *J. Biol. Chem. 271*, 32729−32736.
16. Yang, W., Hendrickson, W. A., Crouch, R. J., and Satow, Y. (1990) *Science 249*, 1398−1405.
17. Keck, J., Goedken, E. R., and Marqusee, S. (1998) *J. Biol. Chem. 273*, 34128−34133.
18. Prorok, M., and Castellino, F. J. (1998) *J. Biol. Chem. 273*, 19573−19578.
19. Jose, T. J., Conlan, L. H., and Dupureur, C. M. (1999) *J. Biol. Inorg. Chem. 4*, 814−823.
20. Huang, H., and Cowan, J. A. (1994) *Eur. J. Biochem. 219*, 253−260.
21. Cowan, J. A., Ohyama, T., Howard, K., Rausch, J. W., Cowan, S. M., and Le Grice, S. F. (2000) *J. Biol. Inorg. Chem. 5*, 67−74.
22. Lai, B., Li, Y., Cao, A.-N., and Lai, L.-H. (2001) *Acta Phys.-Chim. Sin. 17*, 865−867.
23. Chapados, B. R., Chai, Q., Hosfield, D. J., Qiu, J., Shen, B., and Tainer, J. A. (2001) *J. Mol. Biol. 307*, 541−556.
24. Chai, Q., Qiu, J., Chapados, B. R., and Shen, B. (2001) *Biochem. Biophys. Res. Comm. 286*, 1073−1081.
25. Kanaya, S., Oobatake, M., Nakamura, H., and Ikehara, M. (1993) *J. Biotech. 28*, 117−136.
26. Pace, C. N., Vajdos, F., Fee, L., Grimsley, G., and Gray, T. (1995) *Protein Sci. 4*, 2411−2423.
27. Chen, P. S., Toribara, T. Y., and Warner, H. (1956) *Anal. Chem. 28*, 1756−1758.
28. Black, C. B., and Cowan, J. A. (1994) *Inorg. Chem. 33*, 5805−5808.
29. Muroya, A., Tsuchiya, D., Ishikawa, M., Haruki, M., Morikawa, M., Kanaya, S., and Morikawa, K. (2001) *Protein Sci. 10*, 707−714.
30. Danson, M. J., Hough, D. W., Russell, R. J. M., Taylor, G. L., and Pearl, L. (1996) *Protein Eng. 9*, 629−630.
31. Goedken, E. R., and Marqusee, S. (2001) *J. Biol. Chem. 276*, 7266−7271.
32. Leavitt, S.,and Freire, E. (2001) *Curr. Opin. Struct. Biol. 11*, 560−566.
33. Oda, Y., Yoshida, M., and Kanaya, S. (1993) *J. Biol. Chem. 268*, 88−92.
34. Goedken, E. R., and Marqusee, S. (1999) *Protein Eng. 12*, 975−980.
35. Nakamura, H., Oda, Y., Iwai, S., Inoue, H., Ohtsuka, E., Kanaya, S., Kimura, S., Katsuda, C., Katayanagi, K., Morikawa, K., Miyashiro, H., and Ikehara, M. (1991) *Proc. Natl. Acad. Sci. U.S.A. 88*, 11535−11539.
36. Oda, Y., Iwai, S., Ohtsuka, E., Ishikawa, M., Ikehara, M., and Nakamura, H. (1993) *Nucleic Acids Res. 21*, 4690-4695.

BI026960A